Kovove Mater. 54 2016 389–396
DOI: 10.4149/km_2016_6_389

Influence of long-term ageing upon the capacity of hydrogen storage in two novel Mg-Ni-In-C alloys

J. Čermák[1,2]*, L. Král[1], P. Roupcová[1,3]

[1] *Institute of Physics of Materials AS CR, v.v.i., Žižkova 22, 616 62 Brno, Czech Republic*
[2] *CEITEC-Institute of Physics of Materials, Žižkova 22, 616 62 Brno, Czech Republic*
[3] *BUT, FME, IMSE, Technická 2896/2, 616 69 Brno, Czech Republic*

Received 17 December 2015, received in revised form 4 April 2016, accepted 19 May 2016

Abstract

We have shown previously that the addition of In and C enhances the hydrogen desorption capacity and considerably improves the kinetics of hydrogen desorption from Mg-Ni based alloys, important from the perspective of hydrogen storage. In this paper, we present the results of tests of the long-term stability of the sorption behaviour of these materials. We studied how the capacity and sorption kinetics changed 5 years from the preparation of two chosen Mg-Ni-In-C alloys differing in indium concentration. Kinetic curves and PCT isotherms were measured at temperatures of 250–350 °C. It was found that long-term storage of the hydrogen-charged samples led to no significant downgrade in hydrogen sorption kinetics. However, the absorption capacity somewhat decreased from about 5 wt.% H_2 to about 3 wt.% H_2 due to partial phase decomposition. Relatively intensive tentative oxidation during preparation, which had a slightly beneficial effect on the desorption rate of freshly-prepared samples, caused almost total blocking of hydrogen sorption in the aged samples.

Key words: hydrogen, hydrogen storage, magnesium alloys, indium

1. Introduction

Magnesium and its alloys have frequently been studied as light-weight materials for applications where the mechanical strength, creep, fatigue resistivity [1, 2], structure, corrosion, and biodegradability [3, 4] were of prime importance. The materials have also been under investigation for hydrogen storage [5, 6] since hydrogen is a very prospective fuel both for direct combustion and in electrochemical batteries and fuel cells.

The remarkable hydrogen storage capacity of Mg (theoretically 7.7 wt.%) and its low cost still keep Mg-based hydrogen storage materials (HSMs) in the focus of interest, in spite of the relatively high hydrogen sorption temperature and poor sorption kinetics of pure Mg [7]. Series of studies have been devoted to the further improvement of hydrogen sorption kinetics in binary ball-milled Mg-based hydrogen storage (HS) alloys [8–16]. Recently, great attention has been paid to preparation methods and the effect of the size of the Mg particles (see e.g. [17]). Tuning the kinetic properties by catalyst additions [18] is also one of the possible ways to improve the application potential. A high beneficial effect was reported for Ni [19, 20] and some other elements, e.g. Ti [21, 22], Al [23, 24], Nb [25], and Li-containing compositions [26, 27].

In our previous studies [28–32], it was observed that additions of carbon and indium to a Mg-based alloy improved its hydrogen desorption behaviour. It was also shown that the alloy undergoes some ageing/ripening after the initial hydrogen charging [29], which induced a substantial improvement in hydrogen desorption kinetics. A similar beneficial effect of the storage time of Mg-based HSM on the hydrogen sorption characteristics was also reported in [33].

The combined effect of Ni and elements X from the 13th and 14th group was investigated in [30]. It was found that the best results could be achieved when In is introduced into the Mg-Ni base. This was in agreement with the expectation generated by the results reported earlier in [34] for pure Mg. The distribution

---

*Corresponding author: tel.: +420 532290422; fax: +420 541218657; e-mail address cermak@ipm.cz

of X over the phases present in HSM is not uniform. Additive elements X prefer rather the Mg_2Ni phase than the Mg phase and the segregation of X is especially strong in the hydrated phase $Mg_2Ni(X)H_4$, as was reported in [30]. This means that the overall effect of X is mediated by its influence on phase Mg_2Ni.

The beneficial effect of indium on hydrogen sorption was observed first by Mintz et al. [34], where the kinetics of magnesium hydride formation from pure activated magnesium and from some indium-containing magnesium alloys was studied. Improvement in sorption characteristics was recently confirmed in In-containing alloys Mg-Ag [35], Mg-In-Ni [36] as well, and in an experimental survey [14].

In [31], the effect of carbon upon hydrogen desorption in Mg-Ni-In was investigated. The results of that study led to the conclusion that C, ball-milled together with other components, substantially improved the desorption kinetics of the Mg-Ni-In base alloy. However, when the carbon concentration exceeded a certain limit, the phase $Mg_2Ni(In,C)$ decomposed during desorption: in desorbed samples, the In, Ni, and Mg_3In phases were identified by XRD analysis. These products of decomposition are – with respect to hydrogen desorption – less effective. Hence, the sorption cycle (repeated hydrogen charging and desorption) became (partly) irreversible.

It follows that Mg-based alloys containing Ni, In, and C are promising candidates for effective HSMs. In the present work, we tested the HS behaviour of two chosen Mg-Ni-In-C alloys differing in content of In, c_{In}, and with a carbon concentration that was below the limit found in [31] as critical for intensive phase decomposition. The aim of the present study was to assess the influence of c_{In} variation and the influence of long-term ageing upon HS characteristics. We conducted measurements in the sorption regime and studied the stability of A/D cycles. Also, dynamic measurements of formation enthalpy and entropy were carried out.

2. Experimental

Measurements in the present paper were carried out with samples of two alloys that differed in content of indium (wt.%): Mg-16.1Ni-5.2In-9.9C referred to as *Alloy 1* hereafter, and Mg-15.2Ni-9.7In-9.4C referred to as *Alloy 2*. The ratio of the Mg/Ni binary base was chosen below the eutectic point in the Mg-Ni binary alloy system, and the ratio Mg/C was about 7. Samples were ball-milled from pure components (splinters of 3N8 Mg, 3N6 Ni, 5N In, spectroscopic pure C powder – all purchased from SIGMA-ALDRICH) using the ball-mill *Fritsch-Pulverisette6* (450 rpm, 10 min milling/50 min cooling – repeated 20 times; the mass ratio of the balls to the charge was about 60). The powder was compacted at room temperature into pellets that were annealed at 360 °C/20 h/Ar (*Treatment 1*) or 360 °C/20 h in air (*Treatment 2*). *Treatment 2* simulated the kind of harsh handling that might occasionally occur while the HS alloy under examination was in service. Alloys subjected to *Treatment 2* are labelled *Alloy 2-Air*. Ball-milled, compacted and annealed samples were charged by gaseous hydrogen at 345 °C/20 h/30 bar in a pressure vessel. Other details of the sample preparation and measurement arrangement have been described elsewhere [31]. Charged samples of both alloys were stored at room temperature in a well-defined atmosphere of dry air for about 5 years. This storage simulated a long-term service period of HS material.

Hydrogen sorption characteristics were measured using the Sieverts-type gas sorption analyser *PCT-Pro Setaram Instrumentation* in the present work. This equipment enables safe and fully-automated repeated measurements in both absorption and desorption regimes. The study was carried out at temperatures between 250 and 350 °C and under hydrogen pressure from 0.001 mbar to 20 bars. The purity of both the hydrogen and helium (calibration gas) was 6N. The hydrogen was dosed using calibrated volumes corrected to dead volumes at each individual test temperature.

X-ray powder diffraction (XRD) was performed using Cu $K\alpha_{1,2}$ radiation. HighScore Plus software and JCPDS PDF-4 were used for qualitative analysis and Rietveld refinements using external LaB_6 standard and structural models based on the ICSD database for quantitative analysis.

3. Results and discussion

3.1. Sample characterization

After ball-milling, samples consisted exclusively of pure milled Mg and Ni, mechanically alloyed with In. During the annealing (*Treatments 1* and *2*), Mg and Ni formed a mixture Mg(In) + $Mg_2Ni(In)$. XRD phase analysis of charged samples carried out after the ageing led to the conclusion that the Ni-rich phase $Mg_2Ni(In)H_4$ partially decomposed into Ni, In, In_xNi_y, and In_xMg_y. This process was more intensive in *Alloy 2*, with a higher In concentration: the comparison of XRD patterns in Fig. 1 clearly shows the smaller content of $Mg_2Ni(In)H_4$ in *Alloy 2*. The phase composition of hydrogen-charged *Alloy 1* and *Alloy 2*, obtained by Rietveld analysis of XRD patterns, is listed in Table 1.

The structure of alloys was observed by SEM. Typical results are illustrated in Fig. 2, where the structure of *Alloy 2* is shown both in SEI (secondary electrons – Fig. 2a) and in BSE (back scattered elec-

Table 1. Phase composition of hydrogen charged materials obtained by XRD in wt.%; alloys after *Treatment 1*

	Freshly-prepared	Aged, before measurement		Aged, after measurement	
Phase	*Alloy 2**	*Alloy 1*	*Alloy 2*	*Alloy 1*	*Alloy 2*
$Mg(In)H_2$	61.7	71.1	65.6	69.2	64.9
$Mg_2Ni(In)H_4$	28.2	15.0	13.1	26.1	11.2
$Mg_2Ni(In)H_{0.3}$	10.1	7.6	4.7	4.3	20.3
Ni		5.0	14.4		
In		0.4	0.3	0.4	0.6
In_3Mg					1.3
$InMg_3$		0.7	1.6		0.8
$InNi_3$		0.2	0.3		0.9

*Phase composition of freshly-prepared *Alloy 2* taken from previous studies [28–32]; XRD analysis of freshly prepared *Alloy 1* was not done.

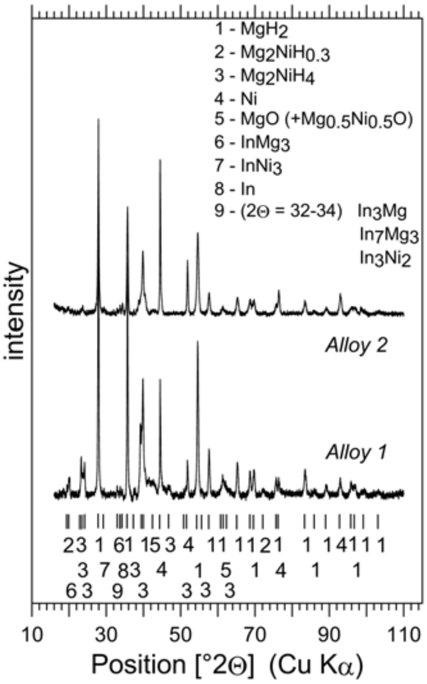

Fig. 1. XRD patterns of *Alloy 1* and *Alloy 2* after long-term storing.

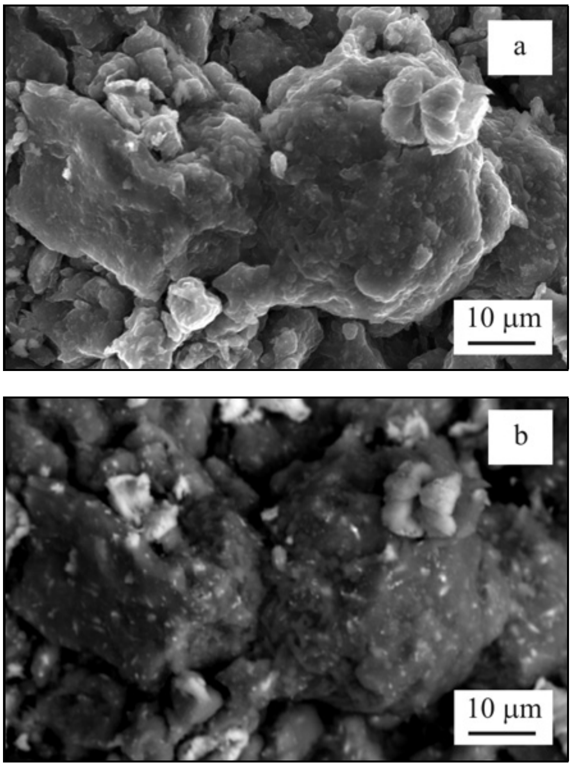

Fig. 2. Typical structure of studied HSMs. SEM image of *Alloy 2*: (a) SE, (b) BSE. Light particles – $Mg_2Ni(In)H_4$ phase.

trons – Fig. 2b) modes. The analysis revealed that hydrogen-charged alloys consisted of large $Mg(In)H_2$ grains, typically between 10 and 60 μm in size, and smaller $Mg_2Ni(In)H_4$ particles, whose grain size varied typically between 0.5 and 30 μm. The smaller $Mg_2Ni(In)H_4$ particles can be seen especially in BSE mode – see the small light particles at the surface of the large $Mg(In)H_2$ grains. In *Alloy 1*, the $Mg_2Ni(In)$ particles are finer (size 0.5–10 μm in size) than in *Alloy 2*, where their size was between 2.5 and 30 μm.

The distribution of elements was observed by EDX in hydrogen non-charged alloys. Typical results can be seen in Fig. 3. It was concluded that In and C tend slightly to segregate in small particles of $Mg_2Ni(In)$.

3.2. Kinetic measurements

Cycling measurements of kinetic curves were done at temperatures between 250 and 295 ℃ with a starting pressure of 20 bars (for absorption) and 0.001 bars (for desorption). The instantaneous hydrogen pressure p in the sample chamber was always well above the equilibrium pressure $p_{eq}(T)$ of the respective hydrides and below the $p_{eq}(T)$ during absorption and desorption, respectively. The maximum number n of A/D cycles in cycling experiments was 10 because it was

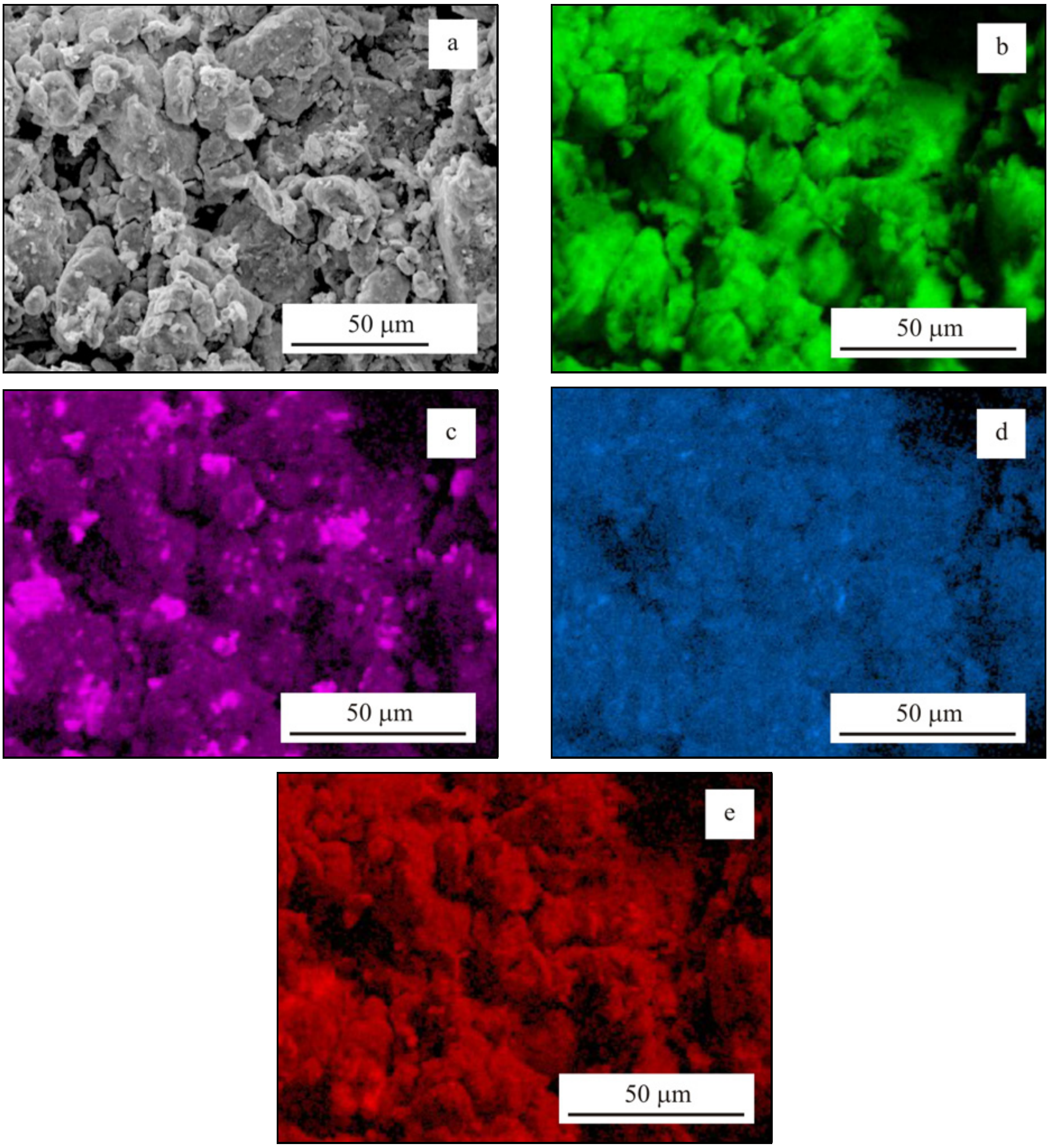

Fig. 3. Typical distribution of elements. EDX mapping of *Alloy 2*: (a) SEI, (b) Mg K_α, (c) Ni K_α, (d) In L_α, (e) C K_α.

proved that this was a sufficient number for stabilizing alloy sorption behaviour in all cases.

In both alloys, the sorption capacity reached approximately 3 wt.% H_2 at 295 ℃, and the cycles were regular. In *Alloy 2-Air*, the sorption capacity was only about 2.5 wt.% H_2; the sorption kinetics was slower and more (about 6) cycles were needed to reach a stable state.

Comparison of sorption curves at both temperatures measured in a well-stabilized state (in the 10th cycle) is shown in Fig. 4. It can be seen that the rate of hydrogen desorption is slightly higher in *Alloy 2* compared to *Alloy 1*, which agrees with the results obtained 5 years ago – see Fig. 5a. It is also obvious that the hydrogen sorption capacity in aged *Alloy 2* is higher than that of *Alloy 1* at a higher temperature (Fig. 4a).

Comparing the time needed for desorption of 90 % of the stored hydrogen (at a test temperature of 250 ℃ used both in the previous and the present studies), one can easily conclude that the hydrogen desorption kinetics remained approximately unchanged after long-term storage of the alloys. However, the hydrogen storage capacity decreased from about 5 wt.% H_2 down to

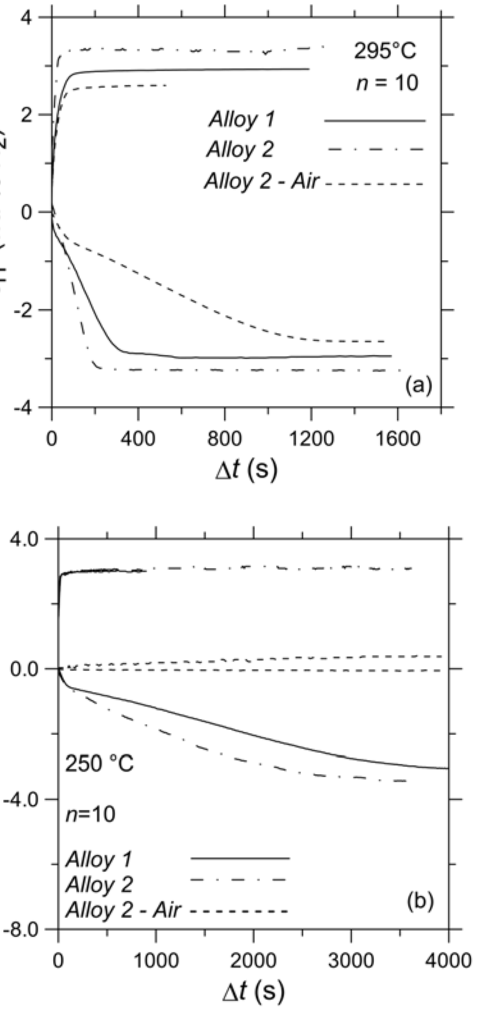

Fig. 4. Sorption curves in a stable state (tenth cycle). Δt is the relative sorption time of the 10th cycle. (a) 295 °C, (b) 250 °C.

approximately 3 wt.% H_2. Such a decrease in capacity can be explained – at least qualitatively – with reference to the lower fraction of hydrogen storing phases (see Table 1): whereas immediately after the first hydrogen charging, only phases effective for hydrogen storage were present ($Mg(In)H_2$, $Mg_2Ni(In)H_4$, and $Mg_2Ni(In)H_{0.3}$), Ni-containing phases partially decomposed after the ageing. It can also be seen that the decay products (Ni, In, In_xMg_y, and $InNi_3$) partly reformed into $Mg_2Ni(In)H_4$ and $Mg_2Ni(In)H_{0.3}$ after cycling measurements with *Alloy 1*. This means that the degradation of the hydrogen storage capacity originates in the partial decomposition of phases able to store hydrogen during long-term storage.

The XRD study resulted in interesting conclusions about the influence of oxidation upon hydrogen absorption (Fig. 4) and desorption (Fig. 5) characteristics: the relatively intensive exposure of *Alloy 2* to the air (*Treatment 2*) caused the formation of MgO, which was kept at a relatively low level by the presence of In. The first desorption tests of *Alloy 2-Air* led to even better desorption kinetics as can be seen in Fig. 5. However, the later sorption tests of *Alloy 2-Air* at 295 °C, carried out in the present work after 5 years, showed considerably reduced hydrogen storage capacity and poor sorption kinetics (Fig. 4a). At a lower temperature, 250 °C, the hydrogen sorption in *Alloy 2-Air* was even almost blocked (Fig. 4b). The beneficial effect of In upon oxidation resistance even after long-term storing can be documented by the XRD patterns in Fig. 1.

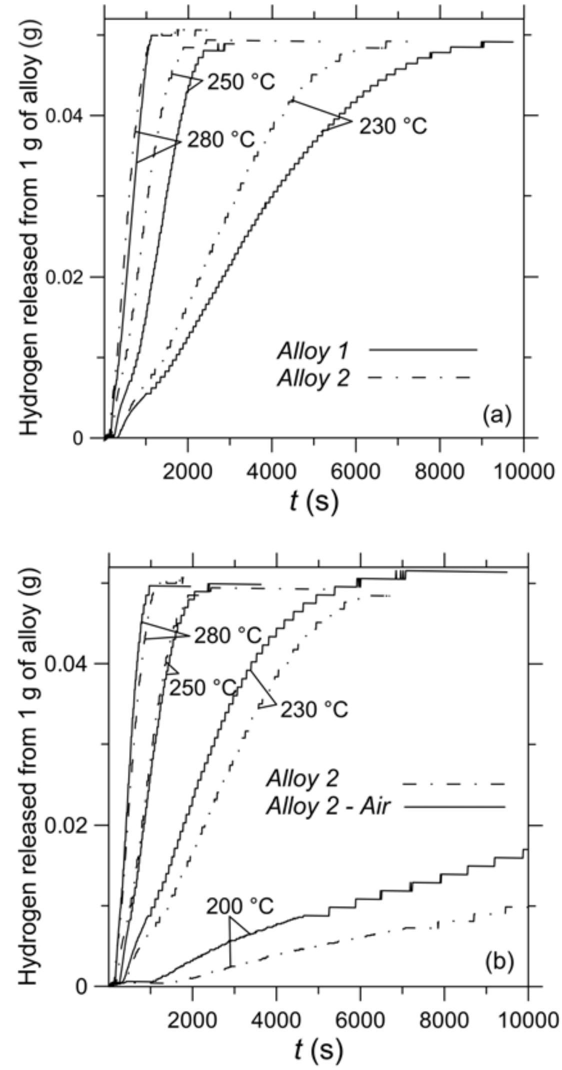

Fig. 5. (a) Comparison of hydrogen desorption curves measured in *Alloy 1* and *Alloy 2* 5 years ago. (b) Hydrogen desorption curves measured 5 years ago – influence of oxidation: *Alloy 2 – Treatment 1*, *Alloy 2-Air – Treatment 2*.

The difference between the relatively rapid hydrogen sorption and poor kinetics of hydrogen desorption (*Alloy 1, Alloy 2* – Fig. 4) is caused, most likely, by different driving forces: the difference in hydrogen

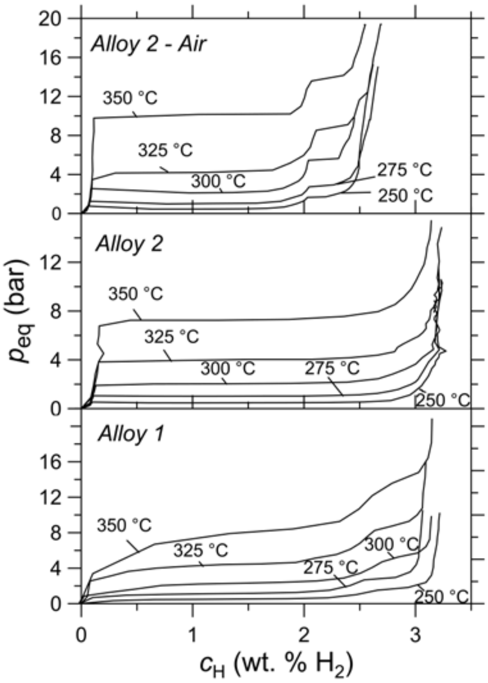

Fig. 6. PCT curves (measured only in an absorption mode).

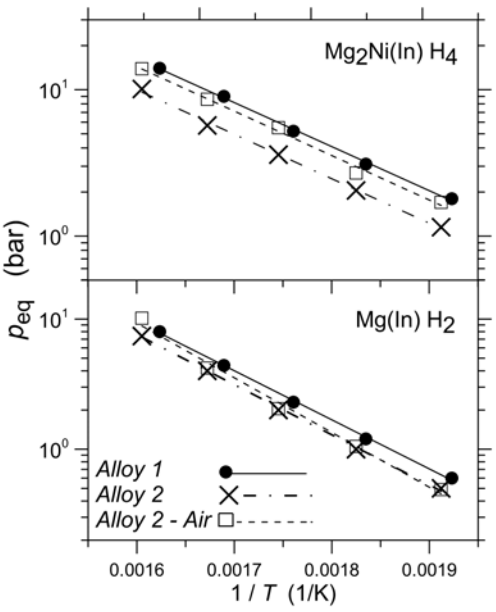

Fig. 7. Van't Hoff diagram.

pressure between the hydrogen reservoir and sample chamber is +20 bars for absorption and –1 bar only for desorption.

The worse sorption kinetics in *Alloy 2-Air* is most likely caused by the oxide phase nucleation during *Treatment 2*, which acted rather as a sorption catalyst in the freshly-prepared samples (Fig. 5b). These oxide particles, once formed, grew relatively easily and formed an oxide layer that could later effectively inhibit hydrogen sorption (Fig. 4b). Reliable evaluation of the amount of oxide phase both in freshly prepared and in aged samples was below the detection limit of XRD.

3.3. PCT isotherms

In Fig. 6, PCT isotherms (dependence of hydrogen equilibrium pressure above the respective hydride, p_{eq}, on hydrogen concentration in solid, c_H, at constant temperature) are compared. All the curves were measured in the absorption regime (some hysteresis can be expected [37], but the absorption mode was chosen as sufficient for relative comparison of the long-term hydrogen behaviour of *Alloy 1* and *Alloy 2*).

The curves show two plateaus – the phase $Mg(In)H_2$ is responsible for the lower one, the short upper plateau reflects the presence of $Mg_2Ni(In)H_4$ hydride [37]. The upper plateau observed in *Alloy 2* is less evident, but temperature-programmed desorption carried out with charged samples proved that both phases were also formed in this HS alloy.

The dependence of dissociation pressure p_{eq} on the reciprocal temperature of the sample is plotted in Fig. 7. The values of p_{eq} were determined at c_H = 1.5 wt.% H_2 for the Mg-rich phase, at c_H = 2.2 wt.% H_2 for the Ni-containing phase in *Alloy 2-Air*, and at c_H = 2.9 wt.% H_2 for the same phase in *Alloy 1* and *Alloy 2*. Formation enthalpies ΔH and formation entropies ΔS are listed in Table 2. It is known that formation entropies of hydride formation ΔS do not vary too much for different hydrides. The present values of ΔS are close to the typical value of $\Delta S \cong 0.13$ kJ mol^{-1} H_2/K [38].

It can be seen that the addition of In very slightly increases ΔH and ΔS in $Mg(In)H_2$ and markedly decreases both Arrhenius parameters in $Mg_2Ni(In)H_4$. This is, most likely, the cause of the partial decay of $Mg_2Ni(In)H_4$ (followed by the decomposition of $Mg_2Ni(In)H_4$ into Ni, In, and $In_x(Mg,Ni)_y$) during long-term storage and its relatively easy restoration during cycling (see Table 1).

To decide whether the observed concentration dependence of the Arrhenius parameters is due to ageing or rather to In addition, *Alloy 2* was once more freshly prepared and annealed according to *Treatment 1*. Arrhenius parameters obtained in the repeated experiment agreed very well with their counterparts measured with aged *Alloy 2* (Table 2). This means that the Arrhenius parameters in the alloys studied are determined by the alloying with In and remain unchanged during long-term ageing.

Table 2. Arrhenius parameters of hydride formation

Alloy	c_{In} (wt.%)	Phase	ΔS (kJ mol^{-1}) H_2/K	ΔH (kJ mol^{-1}) H_2	Remark
pure hydrides	0	MgH_2 Mg_2NiH_4	0.130 0.134	70.8 74.2	Refs. [37, 39]
Alloy 1	5.2	$Mg(In)H_2$ $Mg_2Ni(In)H_4$	0.134 ± 0.002 0.115 ± 0.002	72.2 ± 1.3 57.6 ± 1.3	Aged, this work
Alloy 2	9.7	$Mg(In)H_2$ $Mg_2Ni(In)H_4$	0.135 ± 0.002 0.123 ± 0.009	73.8 ± 1.9 64.0 ± 5.4	Aged, this work
Alloy 2-Air	9.7	$Mg(In)H_2$ $Mg_2Ni(In)H_4$	0.147 ± 0.007 0.115 ± 0.004	80.4 ± 4.2 58.1 ± 2.5	Aged, this work
Alloy 2	9.7	$Mg(In)H_2$ $Mg_2Ni(In)H_4$	0.132 ± 0.002 0.121 ± 0.005	72.4 ± 1.3 64.6 ± 2.8	Freshly prepared, this work

4. Conclusions

The HS characteristics of two prospective HS alloys Mg-Ni-In-C with different In concentration were measured after long-term storage. After 5 years, elapsed from the last hydrogen charging, the A/D cycling tests were performed to assess the behaviour of the material during real service. It was found that:

(i) The beneficial effect of In upon the hydrogen storage characteristics of the alloys studied persisted even after ageing: a higher value of c_{In} leads to better sorption kinetics.

(ii) The formation enthalpy ΔH_{f} of $Mg(In)H_2$ measured with aged alloys seems to be independent on c_{In}, whereas the value ΔH_{f} of $Mg_2Ni(In)H_4$ decreased significantly in alloys with higher content of In. When comparing the values ΔH_{f} for the aged and freshly prepared *Alloy* 2, it follows that the decrease in ΔH_{f} observed in *Alloy* 2 is due rather to In than to ageing.

(iii) Hydrogen storage capacity decreased from about 5 wt.% H_2 in a freshly prepared state down to about 3 wt.% H_2 after ageing.

(iv) A decrease in hydrogen storage capacity was caused by partial phase decomposition of $Mg_2NiH(In)$ H_4. The Ni-containing phase was partially re-formed during the sorption cycles.

(v) The hydrogen sorption in samples that were thermally treated in an oxidizing atmosphere (*Treatment 2*) showed a slight improvement in desorption kinetics in the freshly-prepared state. However, hydrogen desorption was almost blocked after their long-term ageing.

(vi) The results of the present paper suggest that the relatively high hydrogen storage capacity of perspective Mg-Ni-In-C alloys could be kept even after long-term ageing if the phase decomposition of $Mg_2Ni(In)H_4$ into In_xNi and In_x-Mg_y is suppressed. How to reach this goal is a subject of further research.

Acknowledgement

This work was supported by the project CEITEC – Central European Institute of Technology, project number CZ.1.05/1.1.00/02.0068.

References

[1] Avedesian, M. M., Baker, H.: Magnesium and Magnesium Alloys. Materials Park, ASM International 1999.

[2] Paramsothy, M., Nguyen, Q. B., Tun, K. S., Balasubramanian, R., Chan, J., Kwok, R., Kuma, J. V. M., Gupta, M.: Kovove Mater., *49*, 2011, p. 179. doi:10.4149/km_2011_3_179

[3] Smola, B., Stulikova, I.: Kovove Mater., *42*, 2004, p. 301.

[4] Kubasek, J., Vojtech, D., Pospisilova, I.: Kovove Mater., *50*, 2012, p. 415. doi:10.4149/km_2012_6_415

[5] Knotek, V., Lhotka, M., Vojtěch, D.: Kovove Mater., *52*, 2014, p. 345. doi:10.4149/km_2014_6_345

[6] Cermak, J., Kral, L., Stloukal, I.: Kovove Mater., *45*, 2007, p. 305.

[7] Jia, Y., Sun, C., Shen, S., Zou, J., Mao, S. S., Yao, X.: Renewable and Sustainable Energy Rev., *44*, 2015, p. 289. doi:10.1016/j.rser.2014.12.032

[8] Maeland, A. J.: Int. J. Hydrogen Energy, *28*, 2003, p. 821. doi:10.1016/S0360-3199(02)00162-3

[9] Liang, G.: J. Alloys and Compd., *370*, 2004, p. 123. doi:10.1016/j.jallcom.2003.09.031

[10] Maddalena, A., Petris, M., Palade, P., Sartori, S., Principi, G., Settimo, E., Molinas, B., Russo, L.: Int. J. Hydrogen Energy, *31*, 2006, p. 2097. doi:10.1016/j.ijhydene.2006.02.007

[11] Sakintuna, B., Lamari-Darkrim, F., Hirscher, M.: Int. J. Hydrogen Energy, *32*, 2007, p. 1121. doi:10.1016/j.ijhydene.2006.11.022

[12] Shan, J., Li, P., Wan, Q., Zhai, F., Zhang, J., Li, Z., Liu, Z., Volinsky, A. A., Qu, X.: J. Power Sources, *268*, 2014, p. 778. doi:10.1016/j.jpowsour.2014.06.116

[13] Luo, F. P., Wang, H., Ouyang, L. Z., Zeng, M. Q., Liu, J. W., Zhu, M.: Int. J. Hydrogen Energy, *38*, 2013, p. 10912. doi:10.1016/j.ijhydene.2013.03.007

[14] Zhou, C., Fang, Z. Z., Sun, P.: J. Power Sources, *278*, 2015, p. 38. doi:10.1016/j.jpowsour.2014.12.039

[15] Ouyang, L. Z., Cao, Z. J., Wang, H., Liu, J. W., Sun, D. L., Zhang, Q. A., Zhu, M.: Int. J. Hydrogen Energy, *38*, 2013, p. 8881. doi:10.1016/j.ijhydene.2013.05.027

[16] Chen, W., Zhu, Y., Yang, C., Zhang, J., Li, M., Li, L.: J. Power Sources, *280*, 2015, p.132. doi:10.1016/j.jpowsour.2015.01.089

[17] Liu, W., Aguey-Zinsou, K.-F.: J. Mater. Chem. A, *2*, 2014, p. 9718. doi:10.1039/C4TA01108B

[18] Liu, W., Setijadi, E., Aguey-Zinsou, K.-F.: J. Mater. Chem. C, *118*, 2014, p. 27781. doi:10.1021/jp5097663

[19] Cui, J., Liu, J., Wang, H., Ouyang, L., Sun, D., Zhu, M., Yao, X.: J. Mater. Chem. A, *2*, 2014, p. 9645. doi:10.1039/C4TA00221K

[20] Chen, J., Xia, G., Guo, Z., Huang, Z., Liu, H., Yu, X.: J. Mater. Chem. A, *3*, 2015, p. 15843. doi:10.1039/C5TA03721B

[21] Cui, J., Wang, H., Liu, J., Ouyang, L., Zhang, Q., Sun, D., Yao, X., Zhu, M.: J. Mater. Chem. A, *1*, 2013, p. 5603. doi:10.1039/C3TA01332D

[22] Liu, T., Chen, C., Wang, H., Wu, Y.: J. Mater. Chem. C, *118*, 2014, p. 22419. doi:10.1021/jp5061073

[23] Liu, H., Wang, X., Liu, Y., Dong, Z., Cao, G., Li, S., Yan, M.: J. Mater. Chem. A, *1*, 2013, p. 12527. doi:10.1039/C3TA11953J

[24] Liu, H., Wang, X., Liu, Y., Dong, Z., Li, S., Ge, H., Yan, M.: J. Mater. Chem. C, *118*, 2014, p. 18908. doi:10.1021/jp505064s

[25] Zhang, L., Xiao, X., Xu, C., Zheng, J., Fan, X., Shao, J., Li, S., Ge, H., Wang, Q., Chen, L.: J. Mater. Chem. C, *119*, 2015, p. 8554. doi:10.1021/acs.jpcc.5b01532

[26] Li, B., Liu, Y., Li, C., Gao, M., Pan, H.: J. Mater. Chem. A, *2*, 2014, p. 3155. doi:10.1039/C3TA14331G

[27] Gao, M., Gu, J., Pan, H., Wang, Y., Liu, Y., Liang, C., Guo, Z.: J. Mater. Chem. A, *1*, 2013, p. 12285. doi:10.1039/C3TA12472J

[28] Cermak, J., Kral, L.: J. Power Sources, *214*, 2012, p. 208. doi:10.1016/j.jpowsour.2012.04.035

[29] Cermak, J., Kral, L.: Int. J. Hydrogen Energy, *37*, 2012, p. 14257. doi:10.1016/j.ijhydene.2012.07.049

[30] Cermak, J., Kral, L.: J. Power Sources, *197*, 2012, p. 116. doi:10.1016/j.jpowsour.2011.09.045

[31] Cermak, J., Kral, L.: J. Alloys and Compd., *546*, 2013, p. 129. doi:10.1016/j.jallcom.2012.08.037

[32] Cermak, J., David, B.: Int. J. Hydrogen Energy, *36*, 2011, p. 13614. doi:10.1016/j.ijhydene.2011.07.133

[33] Zou, M.-S., Huang, H.-T., Sun, Q., Guo, X.-Y., Yang, R.-J.: Energy, *76*, 2014, p. 673. doi:10.1016/j.energy.2014.08.065

[34] Mintz, M. H., Gavra, Z., Hadari, Z.: J. Inorg. Nucl. Chem., *40*, 1978, p. 765. doi:10.1016/0022-1902(78)80147-X

[35] Si, T., Cao, Y., Zhang, Q., Sun, D., Ouiang, L., Zhu, M.: J. Mater. Chem. A, *3*, 2015, p. 8581. doi:10.1039/C5TA00292C

[36] Lu, Y., Wang, H., Liu, J., Ouyang, L., Zhu, L., Zhang, D., Zhu, M.: J. Mater. Chem. C, *119*, 2015, p. 26858. doi:10.1021/acs.jpcc.5b08984

[37] Schwarz, R. B.: MRS Bull., *24*, 1999, p. 40. doi:10.1557/S0883769400053446

[38] Mooij, L. P. A.: Destabilization of Magnesium Hydride through Interface Engineering. [PhD. Thesis]. Delft, Technical University Delft 2013.

[39] Stampfer, J. F., Holley Jr., C. E., Suttle, J. F.: J. Am. Chem. Soc., *82*, 1960, p. 3504. doi:10.1021/ja01499a006